Invited Paper

Demonstration of two-color transient pumping in Ni-like silver at 13.9 nm and 16.1 nm. New progress in applications of X-ray lasers.

A. Klisnick[1], A. Carillon[1], G. Jamelot[1], P. Jaeglé[1], D. Ros[1], P. Zeitoun[1], F. Albert[1], P. Fourcade[1], J. Kuba[1#], J.-L. Miquel[2], N. Blanchot[2], J.-F. Wyart[3], P. Agostini[4], P. Breger[4], D. Garzella[4], H. Müller[5], D. Joyeux[6], D. Phalippou[6], E. Bechir[7], S. Hubert[7], G. de Lachèze-Murel[7], H. Daido[8]

[1] LSAI, Université Paris-Sud, Bât. 350, 91405 Orsay, France
[2] CEA Limeil, 94190 Villeneuve Saint Georges, France
[3] LAC, Université Paris-Sud, Bât. 505, 91405 Orsay, France
[4] CEA Saclay, DRECAM- SPAM, 91690 Gif-Sur-Yvette, France
[5] FOM Amolf, 1098 Amsterdam, Netherlands
[6] IOTA, BP 147, Université Paris-Sud, 91403 Orsay Cedex, France
[7] CEA BIII, DCRE-SDE, BP 12, 91680 Bruyères-le-Chatel, France
[8] ILE, University of Osaka, Suita, Osaka 565-8577, Japan

ABSTRACT

We present new progress in the optimization and understanding of the transient collisional pumping scheme using an ultra-short sub-ps heating pulse. The effect of traveling-wave irradiation in enhancing the lasing output of the 4d-4p Ni-like Ag line is studied in detail. A new irradiation scheme using a frequency-doubled 600 ps pulse to preform a plasma is tested. Strong lasing is also obtained on a new line at 16.05 nm that we identify to a 4f-4d transition in Ni-like Ag. Finally we review our recent work in the development of applications of the 21.2 nm zinc laser for imaging or exciting matter. New experiments include the probing of a plasma by imaging Fresnel interferometry and a first attempt to demonstrate two-photon ionization in a xenon gas.

Keywords: transient pumping, collisional X-ray lasers, applications, interferometry, multiphoton ionization

1. TRANSIENT PUMPING IN NI-LIKE SILVER

In March 1998, an experiment conducted at LULI and reported at the 6th X-ray laser Conference in Kyoto[1], focused on the extension of the transient pumping scheme to heating pulse with a duration below 1 ps. For such a short heating pulse we demonstrated that traveling-wave irradiation was necessary to observe lasing on the Ni-like J=0-1 4d-4p silver line at 13.9 nm. A time-integrated gain-coefficient of 14.5 cm^{-1} was measured at that wavelength and a saturation-like behaviour of the intensity increase was observed for plasma lengths above 7 mm. This apparent saturation was attributed to a limitation of the amplification length by refraction of the X-ray laser radiation. Refraction was noted to be important in this experiment: the deflection angle of the X-ray laser beam was as high as 13 mrad after traveling in a 1 cm long plasma, whereas in previous experiments using 130 ps pumping pulses[1] the deflection angle of the laser output at 13.9 nm was only 3 mrad, although emitted from a longer, 2 cm plasma. In addition to this large refraction angle the lasing output was noted to exhibit strong angular structures, pointing to the fact that propagation of the amplified radiation in the small active region was not optimum.

also in Faculty of Nuclear Sciences and Physical Engineering, Czech Technical University, Prague, Czech Republic

Part of the SPIE Conference on Soft X-Ray Lasers and Applications III • Denver, Colorado • July 1999
SPIE Vol. 3776 • 0277-786X/99/$10.00

With the aim of improving the propagation of the amplified photons we carried out a new experiment in which the long pulse that is used to preform a plasma was frequency-doubled, while the ultra-short heating pulse was left at the fundamental laser frequency (i.e. $\lambda = 1.057$ μm). In that case the 1ω heating pulse is absorbed at densities below the critical density for the 2ω pulse (see Fig. 1), in a region where the density gradient is expected to be smoother. Another advantage of this 2ω/1ω configuration is that the heating pulse is absorbed in a region which has been properly ionised (up to the Ni-like stage in our case) by the preforming pulse. Thus the heating pulse does not have to create Ni-like ions and its energy is used only to heat the electrons and pump the lasant ions.

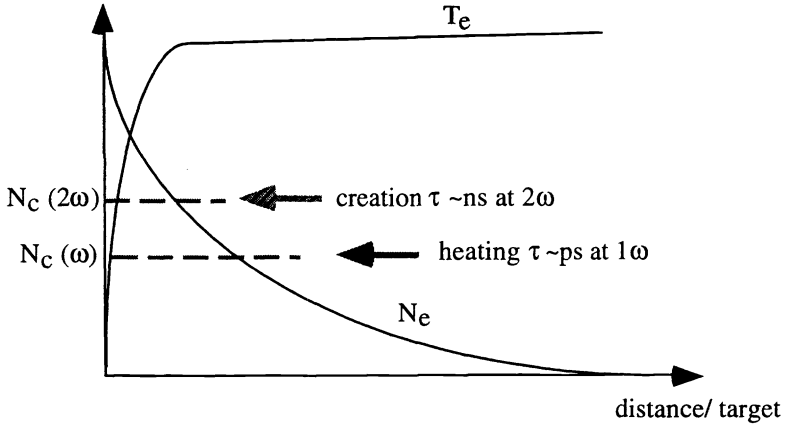

Figure 1: Two-color pumping used in the P102 experiment. The ultrashort heating pulse at 1ω is absorbed at a density which is lower than the critical density of the 2 ω preforming pulse.

The experiment was conducted at the CEA-Limeil in the beginning of 1999, using the P102 CPA laser facility. The plasma was created by irradiating flat silver slabs of 1.50 – 11.80 mm in length with a long 600 ps preforming pulse, followed by a compressed 400 fs heating pulse, both pulses originating from the same stretched and amplified laser pulse. The description of the experimental set-up is given in an accompanying paper[2]. The focusing system used introduces an intrinsic fast traveling wave (TW) along the target at v ~ 6.5 c, where c is the speed of light. The method initially validated in the LULI experiment[3], for generating a TW at the c velocity was thus implemented at P102. This method consists in slightly tilting the second grating of the compressor. This allows to easily control the speed and the direction of the traveling-wave, and also to compensate the intrinsic TW given by the focusing optics, in order to irradiate the target with no TW at all.

The beam carrying the long pulse was frequency-doubled by a KDP crystal with a ~43% efficiency. In the first period of the experiment we varied several parameters in order to find the conditions that optimized the 13.9 nm laser emission. These optimum conditions were: a focal width of 70μm; an energy of ~5 J (at 2ω) in the 600 ps preforming pulse and of ~15 J in the 450 fs heating pulse and a temporal separation of 250 ± 50 ps between both pulses. Unless otherwise specified the results presented below were obtained with these conditions.

The XRL signal was recorded at both ends of the target. A transmission grating spectrometer "SPARTUVIX"[4] provided the time-integrated spectrum with angular resolution in the vertical plane and integration in the horizontal plane over a 3 - 8 mrad interval (according to the adjustment). In the other direction a flat field grating spectrometer (FFS) recorded the time-integrated spectrum with angular resolution in the horizontal plane, and integration in the vertical plane over a ~2 mrad interval. The FFS was thus able to provide information about refraction of the X-ray laser beam in the horizontal plane. This information was used to set the SPARTUVIX spectrometer at the angular peak of emission. For some shots SPARTUVIX was equipped with an XUV streak camera instead of a thinned, back-illuminated CCD, to provide temporal history of the laser emission with a ~5 ps resolution.

1.1 Controlling the X-ray laser output with the travelling wave

The influence of the traveling wave on the XRL intensity was studied in both directions with the two spectrometers. The TW velocity towards the SPARTUVIX spectrometer was set at v = c, while due to technical reasons the velocity in the other direction was at v~1.085 c. However, this difference is not expected to play a significant role.

We examined a triplet of shots at nearly same long and short pulse energies with the following TW conditions: (a) TW towards FFS ($v \approx -c$), (b) without TW (i.e. $v \rightarrow \infty$), and (c) TW towards SPARTUVIX (v = c). Table 1 summarizes the relative intensities measured in both spectrometers for cases (a), (b) and (c). For the FFS spectrometer the 13.9 nm line was not visible above background in case (c) and was very weak in case (b). Thus the relative value given in case (a) of table 1 is only an estimation. It can be seen that both spectrometers indicate that the TW enhances the X-ray laser output by a large factor of ~300-400, compared to the case where the TW is canceled. On the other hand the lasing line intensity is further reduced by a factor of ~0.3 when the TW is directed opposite to the observation. These results are in good agreement with those obtained previously in the LULI experiment when a 0.5 ps pulse was used.

	(a) v = -c	(b) v = ∞	(c) v = c
SPARTUVIX	0.3	1	~417
FFS	~300	1	*

Table 1: Peak intensity values measured at 13.9 nm with each of the spectrometers when canceling (v = ∞) or varying the direction of the TW irradiation.

We also investigated the effect of the TW irradiation on the temporal behaviour of the X-ray laser emission by using a Streak camera behind the SPARTUVIX spectrometer. Figure 2 shows that the duration of the emission at 13.9 nm is significantly shortened when the TW is directed towards SPARTUVIX, compared to the case when the TW is canceled. the duration of the XRL pulse is ~10 ps in the first case and ~15 ps in the second case. Such a duration is close to, although slightly smaller than the 19 ps duration derived from a simple model applied to the LULI experimental results[5].

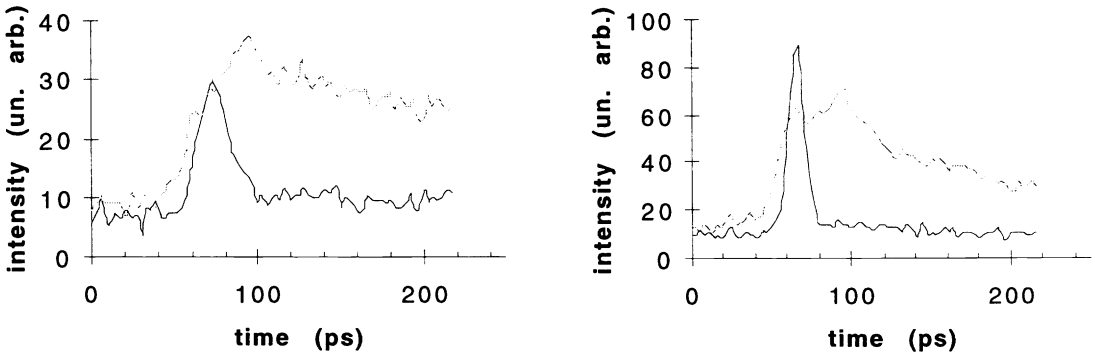

Figure 2: Temporal history of the 13.9 nm laser emission (——) relative to the continuum (- -), obtained from a Streak camera placed behind the SPARTUVIX spectrometer. Left frame: without TW (v~ ∞); right frame: with TW (v=c). The duration of the XRL pulse is significantly shortened when the TW is present. The intensity scales used in each frame are not comparable.

1.2 Characteristics of the 13.9 nm emission

Compared to the previous observations at LULI, the angular distribution of the 13.9 nm was noted to be narrower, 3 mrad FWHM instead of more than 6 mrad. The 2ω/1ω irradiation scheme was actually noted to yield the smallest divergence over all the irradiation schemes tested at P102[2]. On some shots strong angular structures were still observed, indicating that more than one gain region may be produced in the plasma and contribute to the XRL emission.

The deflection angle of the 13.9 nm beamlet was slightly smaller, ~10 mrad instead of ~13 mrad at LULI. However larger values (14 mrad or more) were obtained when the TW was switched off, and when the delay between the preforming pulse and the ultra-short pulse was set to 800 ps instead of 200 ps.

When comprised in the range 3J - 6J no clear influence of the energy of the 600 ps pulse on the 13.9 nm intensity could be found. On the other hand, the 13.9 nm intensity increased exponentially when the energy of the 400 fs pulse was enhanced from 11 J to 16 J.

The gain coefficient was measured with the SPARTUVIX spectrometer by varying the plasma length between 1.5 mm and 11.8 mm. The plot of intensity versus length is displayed in figure 3. An exponential increase corresponding to a gain coefficient (derived from Linford's formula) of 33.5 cm^{-1} is observed for plasma lengths up to 3.8 mm, which then abruptly turns to a linear increase for larger lengths. This saturation-like behaviour was already observed at LULI and is also reported in other transient pumping experiments[6]. However in the LULI experiments the gain coefficient was only 15cm^{-1} and the intensity roll-off was observed for plasma lengths above 7 mm. Thus the maximum gain-length achieved in both experiments is around 12. It is noticeable that a theoretical estimate of the saturation gain-length as well as experiments performed with the « standard » QSS pumping (i.e. with 100 ps pump pulses) produce larger values, of the order of 16. This difference is likely due to the combined effects of saturation and refraction which lead to lower the effective amplification.

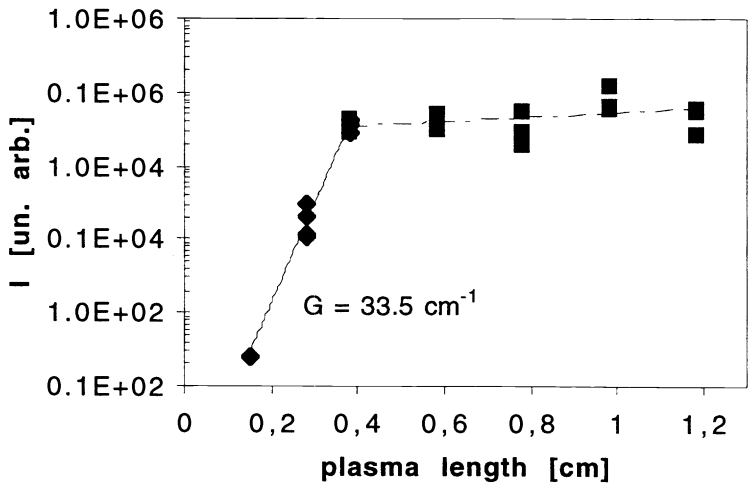

Figure 3: Plot of the time and angle- integrated lasing line versus plasma length. The TW at v=c was directed towards observation.

1.3 Strong lasing line at 16.05 nm

A new lasing line emitted at 16.05 ± 0. 05 nm was observed in this experiment with an intensity that sometimes surpassed the 13.9 nm line. Figure 4 displays a time-integrated spectrum in which the 16.05 nm line and the 4d-4p line exhibit similar intensity. Both lines give rise to a fringe pattern due to diffraction onto the grid supporting the transmission grating. Those satellite peaks actually gave the opportunity to infer the wavelength of the new lasing line from the well-known wavelength of the 4d-4p line. The identification of the 16 nm line to the 4f $^1P_1$ -> 4d $^1P_1$ transition in Ni-like silver was made following recent semi-empirical calculations of energy levels in this ion, performed at L.A.C. (Orsay). These calculations use the Slater-Gordon parametric method with generalized least-square fits[7]. By including several new available experimental

wavelengths, the new calculations gave refined predictions over the formerly published ones[7]. The wavelength of the 4f $^1P_1$ -> 4d $^1P_1$ line is predicted at 15.97 ± 0.1 nm.

The observation of the 4f-4d line with a weak intensity was reported in Ni-like Zr and Mo by the LLNL group[6,8] and interpreted as pumped in part by self photo-pumping from the strong 3d-4f resonance line[9]. Here our observation does not confirm in itself this interpretation but it shows that lasing as strong as on the 4d-4p line can be obtained on the 4f-4d. The lasing output at 16 nm was very unstable from one shot to the other and showed a very high sensitivity to the energy of the short pulse. For this reason we were unable to obtain a reliable measurement of the gain coefficient.

Finally this new line was only observed under specific conditions of irradiation, namely when the TW was directed towards the spectrometer, when the temporal delay between the long and ultrashort pulses was set to 200 ps, and for the 2ω/1ω irradiation scheme. The 4f-4d line never appeared for the other configurations tested (1ω/2ω; 1ω/1ω, see Ref. 2). These indications may help numerical simulations to better understanding the conditions and mechanisms involved in lasing on the 4f-4d.

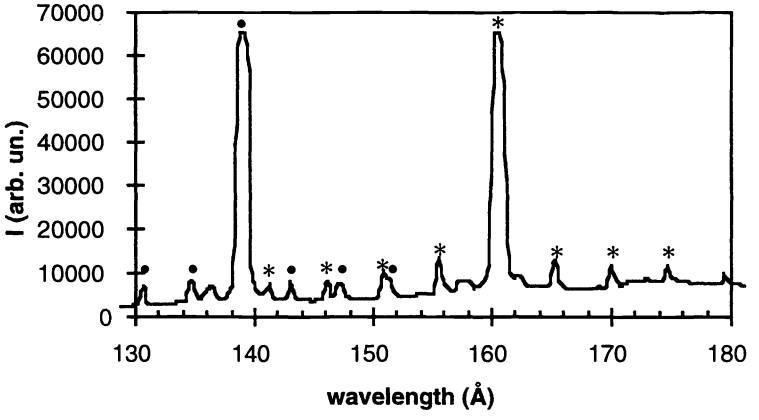

Figure 4: Time-integrated spectrum showing the 13.9 nm line and a strong new line located at 16.05 nm. Both lines give rise to a fringe pattern by diffraction on the grid supporting the transmission grating. These satellite peaks (• and *) are used to infer the peak intensity of the lines when the 0th order saturates the detector. Plasma length 6 mm; TW at v = c towards spectrometer.

2. APPLICATIONS OF THE 21.2 NM ZINC LASER

In this section we report on two recently performed experiments that were aimed at demonstrating new applications of the 21.2 nm zinc laser[10]. This laser operates with a half-cavity mirror which allows to reach a saturated output of ~1 mJ in 80 ps, as well as to significantly increase the spatial coherence of the beam[11]. Previous applications which have been successfully tested include excitation of luminescence in a CsI crystal[12] or probing of surface deformation by Fresnel interferometry[13]. These experiments clearly demonstrated that the high brightness and the energy per pulse now achieved with X-ray lasers allow new investigations that could not be done with other X-UV radiation source.

In our effort to promote the development of applications with X-ray lasers we have been faced to the requirement for a high reliability and reproducibility of the whole system involved in the generation of the X-ray laser source. This concerns in particular the alignment of the half-cavity and the quality and control of the pump laser. To generate the zinc laser we use the six-beam LULI laser facility which delivers a total energy of ~450 J in 600 ps. Strong lasing on the J= 0-1 3p-3s line at 21.2 nm further requires a low energy prepulse (~0. 5 J) preceding the main pulse by 10 ns. We have noted that small unsuspected variations in the spatial profile of the driving laser beam can seriously affect the conditions of operation of the X-ray laser which in turn makes the realization of application experiments sometimes difficult. Thus improving the stability and the reproducibility of the x-ray laser beam from one experiment to the other by a detailed control of all the parameters involved is one of the important task for the future.

The experimental results described below are still preliminary, but they provide a validation of the experimental techniques used and are encouraging first steps for the continuation of the projects.

2.1 Two-photon ionization of xenon with 58 eV laser photons

We present a first attempt to observe two-photon inner-shell ionisation of a xenon gas jet with an X-ray laser. The experiment was carried out at LULI in collaboration with CEA-Saclay and FOM. The source is the Ne-like zinc X-ray laser, emitting at 21.2 nm, which was focused by a spherical multilayer mirror to reach maximum intensity. A time-of-flight electron spectrometer was used to analyze electrons produced by each XRL shot.

Studies of nonlinear laser-matter interaction and multiphoton processes have been so far limited to wavelengths from the near UV to infrared, because of the low brightness of the available sources outside this range. However there is a lot of interest in nonlinear processes in the soft X-ray domain : this would allow to study multiphoton innershell spectroscopy, i.e., the study of atomic transitions forbidden with one photon, XUV nonlinear optics as well as applications of such processes to metrology (for instance autocorrelation measurements of ultrashort XUV pulses).

The observation of multiphoton transitions requires sources of high intensity and coherence. Until now, the observation of two-photon processes was possible only in the case of very low order harmonic generation in gases. For instance, the resonant two-photon ionization of argon at 82.7 nm has been excited by the third harmonic of a KrF laser [14]. In spite of several attempts no successful observation at shorter wavelength has been reported because of the insufficient intensity of the sources. X-ray lasers may thus be the right tool to initiate such investigations.

The removal of an electron from the $4d^{10}$ shell of a xenon atom (ground state configuration is $4d^{10}\ 5s^2\ 5p^6$) requires an energy of 67.5 ($4d_{5/2}$) and 69.5 ($4d_{3/2}$) eV. Then, the absorption of two photons of 58.4 eV (corresponding to $\lambda = 21.2$ nm) is necessary to create a hole. The resulting excited core-hole ion rapidly decays through an Auger process to a doubly charged ion of $5p^4$ ground state configuration, by ejecting a second, Auger- type electron, the energy of which is independent of the incident photon energy. X-ray laser photons also interact with xenon to produce ionisation from the n = 5 shell through more probable one-photon processes. Hence three groups of photoelectrons connected to radiation at 21.2 nm are expected: (i) three peaks at 46.27 eV, 44.96 eV and 35 eV resulting from outer-shell ionisation; (ii) two peaks at 49.25 eV and 47.26 eV resulting from two-photon inner-shell ionisation and (iii) several peaks between 33 and 36 eV resulting from Auger processes.

The values of the cross-section for the two-photon ionization of the xenon 4d levels are unknown, but an order of magnitude was evaluated from the well-known cross sections corresponding to one-photon ionisation to the $4d^9$ np (n>5) levels. We find that the cross-section for the two-photon process is at least of the order of 5. 10^{-49} cm^4.s. Based on this cross section we estimated that the number of 21.2nm laser photons that could be focused in the interaction region was high enough to induce a detectable signature of the two-photon ionization. This estimation was based on the previously measured characteristics of the zinc laser[10] and an expected focal spot of 10 μm x 10 μm.

Figure 5 shows a schematic view of the experimental set-up. The 21.2 nm zinc laser, operated in double-pass, was focused in the vacuum interaction chamber of a time-of-flight electron spectrometer by a spherical multilayer mirror (Mo:Si, R = 7 cm, 30% reflectivity at 21.2 nm) used on-axis. The distance between the X-ray laser plasma output and the mirror was of 1.4 m. A collimation slit was set at the entrance of the spectrometer in order to prevent the incident X-ray laser beamlet to generate unwanted electrons through interaction with the metallic poles of the magnetic bottle spectrometer. Moreover the experimental design included a nylon wire (diameter 300 μm) that was set across the slit to protect the interaction zone from incident X-ray (laser or thermal) photons, in such a way that only those photons at 21.2 nm reflected by the mirror could reach the interaction region.

A gas injector was used to provide xenon atoms at a density of ~10^{14} cm^{-3} in the interaction chamber. This chamber was separated from the time-of-flight region by a pinhole that allows to keep a pressure lower than 10^{-4} Torr, acceptable for the multichannel plate detector.

In the first part of the experiment the wire had to be removed to allow a precise alignment of the X-ray laser axis relative to the small (~2 mm x 0.3 mm) interaction region. Figure 6 shows an example of a footprint of the X-ray laser beam obtained through the spectrometer (for this shot the focusing mirror was removed). The 21.2 nm laser beam is well centered relatively to an alignment point which located the center of the interaction region. Unfortunately we did not get enough time before the end of the run to set the wire back and all the preliminary results were obtained without it.

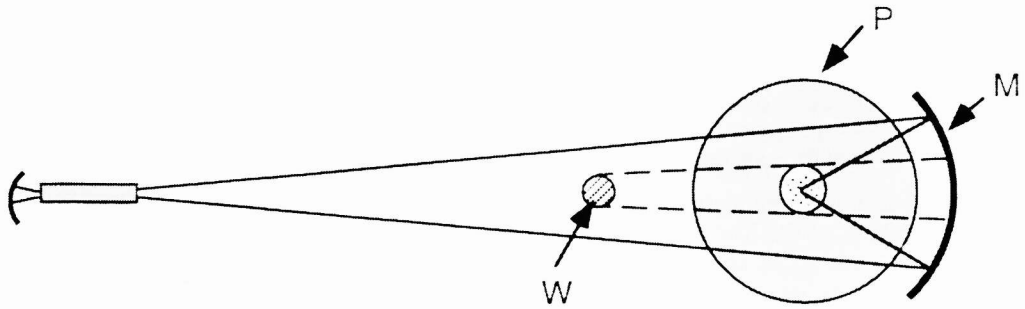

Figure 5: Side-view of the experimental set-up: the X-ray laser beam is focused in the interaction region of a magnetic-bottle electron spectrometer (one of the pole P is shown) by an XUV spherical mirror (M). A nylon wire (W) is set on the beam path to prevent irradiation of the xenon gas by unwanted photons.

Figure 6: Footprint of the 21.2 nm laser beam taken at 2 m from the source, behind the electron spectrometer. The laser beam appears in white in the image and the shadows of several objects set on the beam path appear in black: the collimating slit, the alignment point, and cross-wires. Such a footprint was used to verify the alignment of the X-ray laser beam relative to the interaction region.

Figure 7 shows a typical electron spectrum obtained: the strongest structures are observed at about 400 eV. These structures were interpreted as due to thermal keV radiation emitted by the plasma that ionized xenon in the 3d shell. This radiation should have been stopped by the wire if present. The 1 keV radiation is also responsible for the broad weaker structures observed between 30 and 80 eV (ionisation of the 3p shell). These structures could have masked the 2-photon ionisation lines that lie in the same energy region. A new experimental set-up is now under study that will have to allow the filtering of unwanted radiation while keeping the axis free for the alignment of the X-ray laser.

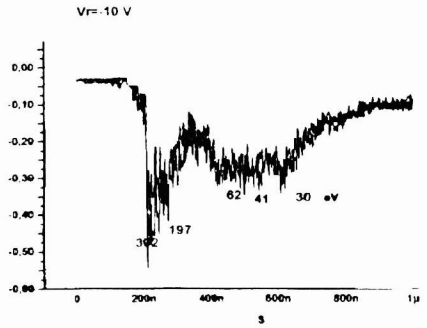

Figure 7: Example of electron spectrum obtained with the time-of-flight spectrometer (time is along horizontal scale) when the X-ray laser beam was focused in xenon. The spectrum is dominated by strong structures at high energy, induced by keV thermal emission from the plasma. These structures potentially mask the two-photon signature.

2.2 Imaging Fresnel interferometry for dense plasma probing

Using the 21.2 nm laser as a source a wavefront interferometer based on a Fresnel bimirror was successfully used for probing of surface defects[15]. In order to apply this kind of interferometer to the probing of dense laser produced plasmas the design was modified so as to provide interferograms with a higher spatial resolution. The first experiment of plasma interferometry with an X-ray laser was performed at LLNL[16]. It used an amplitude-division Mach-Zehnder interferometer combined to the Ne-like yttrium laser at 15.5 nm. The short wavelength of X-ray lasers associated with interferometry technique is expected to provide new information about the structure of the dense part (Ne~ 10^{22} cm^{-3}) which cannot be sampled with usual interferometry at longer (UV) wavelength.

A general schematic view of our experimental set-up is shown in figure 8. One half of the 21.2 nm laser beam goes through a sample plasma while the other part serves as a reference beam. The plasma is placed at a distance of 2.8 m from the source output. This distance was chosen as a good compromise between maximising the spatial coherence of the beam and keeping the intensity high enough to produce detectable interference fringes.

The X-ray laser beam then enters the imaging interferometer which consists of a Fresnel bimirror that deviates the two half X-ray laser beamlets and an imaging multilayer mirror (Mo:Si, R= 999.9 nm) used in quasi-normal incidence. This mirror was aspherized in the vertical direction in order to correct for astigmatism. Note that compared to the previously used Fresnel interferometer the bimirror produces diverging instead of converging XRL beamlets. Hence the interference field where the two half-beams overlap is virtual.

The two optical components are accurately adjusted so that the object plane of the imaging mirror contains the sample plasma and the virtual interference field. The image of this object plane is recorded with a magnification of ~ 9 onto a cooled-, thinned-, back-illuminated CCD that was positioned at a distance of 5.18 m away from the imaging mirror. The expected spatial resolution is of 5 μm over a field of ~700μm in the object plane. In this configuration the direction along the interference fringes correspond to the main expansion axis of the sample plasma.

The X-ray laser plasma, sample plasma and interferometer were placed in three distinct vacuum interaction chambers connected by tubes. Five of the six-beam LULI laser were used to generate the 21.2 nm laser while the sixth laser beam was used to create the sample plasma.

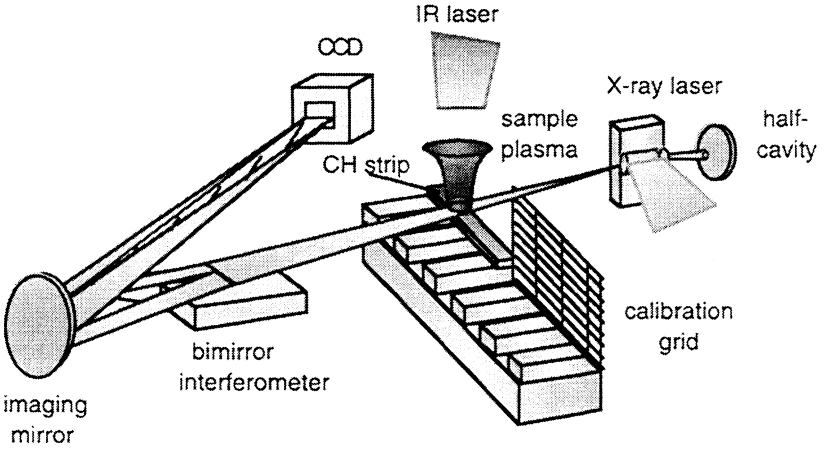

Figure 8: Artist-view of the experimental set-up: after probing the sample plasma the X-ray laser beam is separated into two diverging half-beams. The virtual interference field and the sample plasma are accurately set in the object plane of the imaging mirror. The magnified image of the interferogram is recorded on a cooled, back-illuminated CCD. The target mount was designed to support CH strips that could be irradiated and a calibration grid to test the spatial resolution achieved.

In order to determine the actual resolution achieved by the imaging interferometer, a first image by illuminating a calibration grid with the 21.2 nm laser through the interferometer. This grid was set at the position of the sample plasma. The thickness of the grid bars was of 7μm and the spacing between bars was of 25μm. A detail of the obtained image is

displayed in Fig. 9. The spatial resolution achieved is of 4 μm which confirms the very high quality of the corrected imaging mirror used.

First reference interferograms (i.e. without sample plasma) were then obtained, an example of which is presented in figure 10. One can see that interference fringes with a good visibility are obtained over the whole aperture. The field sampled by the interferometer is 700μm in horizontal and ~1mm in vertical (in the object plane).

Finally we performed a few shots with the sample plasma. This plasma was created by focusing one of the six LULI laser beam on a structured aluminum target that had been initially designed to support CH strips. Due to a small misalignment of the target, the densest part of the sample plasma was masked and no fringe shift could be clearly detected. However the interferograms as well as the mesh image obtained validate the capability of the interferometer. New experiments are planned in 2000 that will be carried out at the Gekko XII facility in collaboration with the group of H. Daido at ILE.

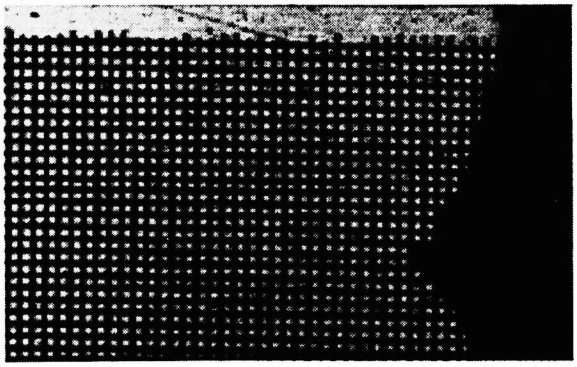

Figure 9: Detail of an image of the calibration grid obtained at 21.2 nm through the imaging interferometer. A spatial resolution of 4μm is achieved. Grid bars are 7μm thick and 25μm spaced.

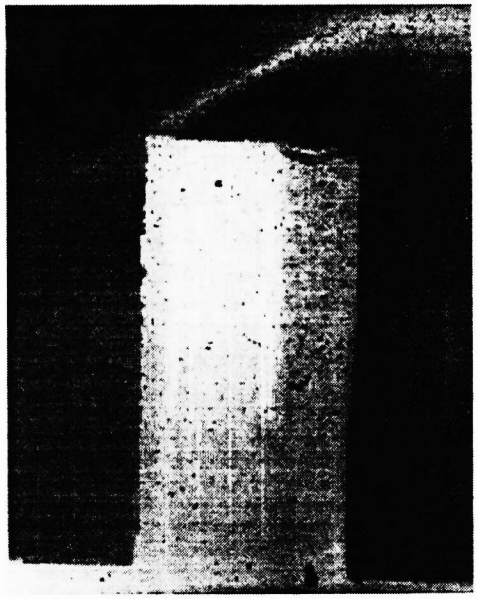

Figure 10: Reference interferogram obtained with the zinc laser (no sample plasma). The dark area is the shadow of the structured target mount (see Fig. 8). The field sampled by the interferometer is 700μm in horizontal and ~1mm in vertical (in the object plane).

3. CONCLUSIONS

With the aim of improving the propagation of X-ray lasers pumped in the transient regime we tested a two-color irradiation scheme in which the preforming pulse is at a shorter wavelength than the ultrashort heating pulse. A large gain of 33.5 cm^{-1} is obtained on the Ni-like Ag 4d-4p line at 13.9 nm with a modest energy requirement on target of 3J/cm and 7.5 J/cm in the long and short pulse respectively. The divergence of the X-ray laser beamlet is substantially improved over the previous experiment performed at LULI with a 1ω irradiation (3 mrad instead of 6 mrad). However the deflection angle is still large (~10 mrad), indicating that refraction strongly affects the propagation of the amplified photons.

The effect of travelling wave irradiation on the output lasing signal at 13.9 nm was investigated in detail. A x300-400 enhancement factor was observed when a TW running at v=c was applied to the 400fs heating pulse. This enhancement could be observed in the two opposite directions by controlling the direction of the TW. With the TW a shortening of the duration of the X-ray laser pulse to ~10 ps was noted on the time-resolved spectra obtained with a ~5 ps resolution Streak camera.

Finally a new lasing line at 16.05 nm was observed under specific irradiation conditions, with an intensity which sometimes surpassed the 13.9 nm line. Following semi-empirical calculations we identify this line to the 4f $^1P_1$ -> 4d $^1P_1$ transition in Ni-like silver. The understanding of the plasma conditions that favour strong lasing on this line and of the potential role of photopumping requires further investigation.

Preliminary results were obtained in two new application experiments involving the 21.2nm zinc laser. A first attempt of inducing two-photon inner-shell ionisation of xenon was carried out. The electron spectra obtained were dominated by strong structures due to the interaction of thermal keV plasma emission with the xenon atoms. Those structures prevented the detection of a potential signal of two-photon ionisation induced by X-ray laser. A modification of the design of the experimental set-up is under study and next experiments should be carried out in 2000.

First interferograms were obtained with a new Fresnel imaging interferometer which was designed to allow probing of the dense part of laser plasmas with a high spatial resolution. This interferometer includes a spherical multilayer mirror which was corrected for astigmatism and a bimirror for overlapping of half-parts of the X-ray laser beam. A high spatial resolution of 4μm in the object plane was experimentally demonstrated. First interferograms were obtained at a distance of ~8.5 m from the source with a good visibility, thus validating the instrument. New experiments will be performed at ILE (Japan) on the Gekko XII facility, using the 13.9 nm Ni-like silver laser[17].

Acknowledgments:

For the P102 experiment we gratefully acknowledge the technical assistance of I. Legoff, A. Pierre, A.-M. Couvret and G. Lidove (CEA-Limeil), and calculations relevant to the implementation of the TW, provided by J.-C. Chanteloup (LULI). We also acknowledge fruitful discussions with S. Jacquemot (CEA-B3). We thank J.- C. Lagron and L. Vanbostal for their contribution in the design and build-up of the application experiments described in this paper. The construction of the imaging interferometer was financially supported by an ULTIMATECH contract. Finally we acknowledge the valuable contribution of R. Mercier (I.O.T.A.) who realized a corrected imaging mirror of high quality.

REFERENCES

[1] A. Klisnick et al., X-Ray Lasers 1998, IOP Conf. Series N°**159** (1999) 107

[2] J.-L. Miquel et al., This Conference

[3] J.-C. Chanteloup et al., X-Ray Lasers 1998, IOP Conf. Series N°**159** (1999) 653

[4] J.-L. Bourgade et al., Rev. Sci. Inst. **59** (1988) 1840

[5] A. Klisnick et al., submitted to Phys. Rev. Lett., May 1999

[6] J. Dunn et al. X-Ray Lasers 1998, IOP Conf. Series N°**159** (1999)51

[7] J.F. Wyart, Phys. Scr. **36** (1987) 234

[8] Y. Li et al., Phys. Rev.A **58** (1998) R2668

[9] J. Nilsen, J.O.S.A. B **14** (1997) 1511

[10] B. Rus et al. *Phys. Rev. A* **55** (1997) 3858

[11] O. Larroche et al., This Conference

[12] P. Jaeglé et al., *J. Appl.Phys.***81** (1997) 2406

[13] P. Zeitoun et al., *Nuclear Instruments and Methods A* **416** (1998) 189

[14] D Xenakis, O Faucher, D Charalambidis and C Fotakis, J Phys B, **29** (1996) L457

[15] F. Albert et al., *Opt. Comm.* **142** (1997) 184

[16] A. S. Wan, et al., Phys. Rev. E, **55** (1997) 6293

[17] S. Sebban et al., X-Ray Lasers 1998, IOP Conf. Series N°**159** (1999) 91